Quest Journals
Journal of Research in Environmental and Earth Sciences
Volume 11 ~ Issue 5 (May 2025) pp: 39-49
ISSN(Online) :2348-2532
www.questjournals.org

Research Paper

Quiet-time Geomagnetic Field Variations Computed from Spherical Harmonic Coefficients and Mantle Conductivity Profile over Asia Sub-region

Abbas Mustapha[1], Mukhtar Ibrahim Furfuri [2], Mohammd Bello Kaoje [2]
Mukhtar Mohammad [3] Yusuf Aminu Koko [*1] Aminu Mohammad [1*]
Yoshikawa Akimoto [4*]

[1] *Department of Physics, Kebbi State University of science and Technology, Aliero, Nigeria*
[2]*Federal College of Education Technical, Gusau, Zamfara State*
[3]*Federal University of Agriculture, Zuru, Kebbi State, Nigeria*
[4]*International Center for Space Weather Science and Education (ICSWSE), Kyushu University, JAPAN*

ABSTRACT
The study used quiet magnetic field records to study the external, internal and sum of the Sq field variations during extremely quiet year 2008 in Asian sub-region. Spherical harmonic analysis (SHA) technique was used to separate the external and internal Sq field contributions. The result shows that the daytime external $MSqH_{ext}$, internal $MSqH_{int}$, and sum $MSqH_{Tot}$ equator-ward (pole-ward) of the Sq focus are bounded by eastward (westward) current that decreases (increases) with increasing latitudes. The $MSqD_{ext}$ shows a noticeable absence of northward (southward) current flow during the pre-noon (afternoon) periods at LKW suggesting possible cancelation of the meridional current effect. The slight phase changes associated with variable pattern in $MSqZ_{int}$ suggest likely electromagnetic induction effect. The coefficients of the external and internal parts of the quiet geomagnetic field of the stations and the application of Schmucker's equivalent substitute conductivity method allowed for the determination of conductivity profile to a depth of about 700 km. The profile shows existence of weak conductivity ~ 0.015 S/m at depth range ~40 and 100 km and also 200-280 km. At greater depth, the profile shows an exponential increase indication of possible change in mineral composition bound this region. The profile also shows an evidence of discontinuity at depth ~380-460 km. The conductivity profile reveal various phases of mineral composition and transformation thus indicates lateral inhomogeneous layer bound the Asian sub-region in contrast to the earlier models that reported lateral homogeneous layer
Keywords: *Magnetic field, Electric field, ionosphere, Solar quiet (Sq) current, Conductivity*

Received 12 May., 2025; Revised 20 May., 2025; Accepted 22 May., 2025 © The author(s) 2025. Published with open access at ***www.questjournas.org***

I. Introduction

On quiescence days, the magnetic field records obtained below the aurora latitude (±70°) variation usually display a smooth regular daily occurring pattern and this phenomenon is called solar quiet variation or simply "Sq variations" [1]. [2] defined the Sq field variation as field that systematically changes with local time of the day. The magnetic field records at any observatory across the globe are a combined effect of two main current systems. One originates from the dynamo currents (external source current) located at an altitude between ~ 90-150 km in the ionosphere and the other is the induced current (internal source current) from the conductive solid Earth [3].The application of spherical harmonic analysis (SHA) helps in separating the external and internal contributions [4]. This has help in identifying that the observed Sq variations at the ground surface come mainly from external source with little contribution from the induced current, [3, 5].

The Sq field variation is generated by current in the E-region of the ionosphere when thermotidal wind of global scale transports conductive charged particles across the Earth's main field [1, 6]. For each particular day, the Sq field variations are associated to two equivalent current loops, located in each hemisphere during the sunlight hours [6, 7]. The current vortex flows clockwise (counter-clockwise) in the southern (northern) hemisphere. The centre of these currents loops is known as the Sq focus of the current loop.

Several studies have been carried out to examine the characteristics of the external and internal field variations e.g., [8, 9]. These studies revealed significant day-to-day variability of the pattern, magnitude and focus location of the Sq current loop in addition to its seasonal and solar cycle dependence. Several studies in the past and in recent times have pointed out that the intensity of the Sq field variations is stronger (weaker) in summer (winter) hemisphere [1, 10]. The summer current system has been reported to penetrate into the winter hemisphere indication of eminent penetration of the summer field into the winter hemisphere [10]. [11] Observed that the Sq equivalent current field appeared stronger (weaker) in summer (winter) and the mean intensity of the sq current exhibit semi-annual variation in both hemispheres. [10, 12, 13] attributed the seasonal variations of Sq current to inter-hemispheric field aligned currents (FACs).

Most of the earlier and recent studies have focused on the Sq equivalent current composed of external and internal currents systems. These studies have used spherical harmonic analysis (SHA) technique to study the characteristics of the external and internal current systems e.g., [7, 14, 15, 16] but the associated external and internal Sq field has not been given adequate attention, hence knowledge on the external and internal field remain elusive. In this present study, attempt has been made using the spherical harmonic analysis (SHA) technique to characterized the external and internal Sq field variations during period of dip minimum solar activity. The SHA coefficients of the external and internal parts of the Sq field variations of the orthogonal components across the stations were further used to estimate the mantle electrical conductivity over Asian sub-region. Hence, on this note, we present the data selection and analysis technique in section 2 and the results are presented in section 3. We discussed the results in section 4 and draw conclusion in section 5.

II. Materials and Methods

2.1 Data and Analysis Procedure

The magnetic field records in this study consist of the minute average records of the three orthogonal (H, D and Z) components in Asian sub-region during the quietest year 2008. The data were obtained by Magnetic Data Acquisition System (MAGDAS). Table 1 provides the lists of the magnetic observatories and their coordinate systems used in the study. Even though the year 2008 appeared to be the quietest year in recent history, only days with Kp≤3 are used in the study. The set of data for each orthogonal component are averaged to hourly values and the concept of local time was used throughout the analysis.

Table 1. List of MAGDAS data stations and their coordinates system used in the study

		Geographic		Geomagnetic
Name	Code	Lat (°N)	Lon (°E)	Lat (°N)
Langkawi	LKW	6.30	99.78	-3.30
Manado	MND	1.44	124.84	-7.80
Kupang	KPG	-10.20	123.40	-19.58
Rockhamp	ROC	-23.19	150.31	-32.40
Crib Point	MLB	-38.36	145.18	-49.46
Macquarie Island	MCQ	-54.50	158.96	-64.54

A spherical harmonic analysis (SHA) technique was applied for each orthogonal component at each latitude location. Spherical harmonic coefficients of the field variations for each month were determined. The analysis which successfully modelled an opposite hemisphere field variation from that of the primary region generate a set of spherical harmonic coefficients which were used to generate the external and internal composition of the geomagnetic field variations. The separated Sq current generated from the analysis procedure was further used to probe the electrical conductivity-depth profile of the Asian sub-region. The details of the analysis techniques are given in [17, 18].

2.2 Upper Mantle Conductivity

Schmucker was the first to profile the conductivity of the Earth's interior using a transfer function that utilizes the internal and external harmonic coefficients for a given location as input parameters [19]. [20] generalized the Schmucker's transfer function using a set of complex mathematical procedures as shown below;

$$C_n^m = Z - iP \qquad (1)$$

Equation 1 consists of two principal components; a complex real part Z and an imaginary –P part that are defined as;

$$Z = \frac{R}{n(n+1)}\left\{\frac{A_n^m\left[na_n^{me}-(n+1)a_n^{mi}\right]+B_n^m\left[nb_n^{me}-(n+1)b_n^{mi}\right]}{(A_n^m)^2+(B_n^m)^2}\right\} \quad 2a$$

$$P = \frac{R}{n(n+1)}\left\{\frac{A_n^m\left[nb_n^{me}-(n+1)b_n^{mi}\right]-B_n^m\left[na_n^{me}-(n+1)a_n^{mi}\right]}{(A_n^m)^2+(B_n^m)^2}\right\} \quad 2b$$

Where R (km) is the radius of the Earth, the Z and P are also given in kilometer and the coefficients sum are expressed as;

$$A_n^m = (a_{ex})_n^m + (a_{in})_n^m \quad 3a$$

$$B_n^m = (b_{ex})_n^m + (b_{in})_n^m \quad 3b$$

For each (m, n) set of coefficients, the depth to the uniform substitute layer is given as;

$$d_n^m = Z - P \text{ (km)} \quad 4a$$

and has a uniform substitute –layer conductivity (S/m) given as;

$$\sigma_n^m = \frac{5.4 \times 10^4}{m(\pi P)^2} \text{ (Sm}^{-1}) \quad 4b$$

The ratio S_n^m of the internal to the external components of the geomagnetic surface field is express as;

$$S_n^m = u + iv \quad 5a$$

where

$$u = \left[\frac{(a_n^{me})(a_n^{mi})+(b_n^{me})(b_n^{mi})}{[(a_n^{me})]^2+[(b_n^{me})]^2}\right] \quad 5b$$

$$v = \left[\frac{(b_n^{me})(a_n^{mi})-(a_n^{me})(b_n^{mi})}{[(a_n^{me})]^2+[(b_n^{me})]^2}\right] \quad 5c$$

The cogency of equations 4a and 4b is limited by three conditions. The first condition is given as;

$$0° = \arg(C_n^m) \geq -45°; \quad 6a$$

The second condition is that;

$$80° \geq \arg(S_n^m) \geq 10.5°; \quad 6b$$

The third condition is given as;

$$[(A_n^m)^2 + (B_n^m)^2]^{0.5} \geq G_m \quad 6c$$

Equations 6a and 6b are basically applied to resolve any likely outliers in the data and any possible smaller amplitude in the SHA coefficients that may cause poor conductivity estimates. The value of G_m is taking arbitrary for every m data set, and $G_m = 0.5$ was found to give the best estimate. We extend the value of G_m to be 0.5 ($G_m = 0.5$) and found the conductivity-depth decreases and subsequently remove higher m components that are by nature of the source current of lower amplitudes [21].

A schmucker's transfer function was then applied for the determination of the conductivity values for each particular location with the external and internal SHA coefficients representative of that site [19]. In this study, the SHA coefficients arise from the fitting of a potential function representative of a smoothed Fourier component of the Sq field obtained in the Asian sub-region. Highest potential function was obtained at the Sq current focus latitude indication that this region dominates the SHA coefficients determination. When the focus moves through the year, the main contribution of the potential function comes from slightly different configuration of the potential function. The potential function that is composed of polynomial with odd values (n-m) represent the Sq systems with similar current foci locations in the opposite hemisphere [19]. In this study, we use the odd (n-m) terms to estimate the depth and this process assure a more unique latitude sampling of the conductivity-depth determination. The conductivity σ and depth d values for equivalent substitute conductors were determined using equation 2a to 4b. To avoid effect of horizontal irregularities in conductivity as the current focus location changes through the year, the σ, and d values for a given n and m were carefully smoothed using a locally weighted robust regression fitting [22].

III. Results

The magnetic field records for the year 2008 are used in the present study. The solar magnetic activity for this year are quite minimal, in fact it's the quietest year in recent history with an annual sunspot number R_z = 3.9 which makes it more appropriate to characterized the variability features of the Sq field and also to estimate the mantle electrical conductivity profile beneath the Asian sub-region. The external and internal harmonic coefficients determined in each month using spherical harmonic analysis allowed us to reconstruct the monthly external and internal fields for each orthogonal component (H, D, and Z).

Figures 1 to 3 illustrate the monthly latitudinal profile of the external, internal and sum (external plus internal) of the quiet Sq fields reconstructed from the SHA coefficients. The field provides quantitative contributions of the external and internal field and the source mechanism responsible for the variability of the phase and intensity of the Sq current systems responsible for the quiet fields. It is conspicuously seen in Figure 1 (panel H1) that the external horizontal field $MSqH_{ext}$ is bounded by night-time (17:00-06:00 LT) hrs negative amplitude at LKW, MND and KPG latitudes. During these periods, positive $MSqH_{ext}$ magnitudes were observed at the latitudes of MLB and MCQ. Apart from these night-time variations, the $MSqH_{ext}$ are characterized by daytime (07:00-16:00 LT) hrs positive amplitudes apparently seen at LKW and MND latitudes with a substantial decrease that is accosted by a phase shift at ROC latitudes. The daytime, maximum positive $MSqH_{ext}$ reached $\sim$ 30 nT at LKW in May as depicted in Figure 1 (panel H1). The daytime positive $MSqH_{ext}$ magnitude occurred between 10:00 and 11:00 LT hrs and thus reflects the marked effect of solar activity. At latitudes beyond ROC $MSqH_{ext}$ exhibit daytime negative amplitudes that seem to increase with increasing latitudes. The daytime negative $MSqH_{ext}$ magnitudes reached ~ -25 nT in February at MCQ latitude. These negative $MSqH_{ext}$ peak amplitudes are mostly observed around (11:00-12:00 LT) hrs.

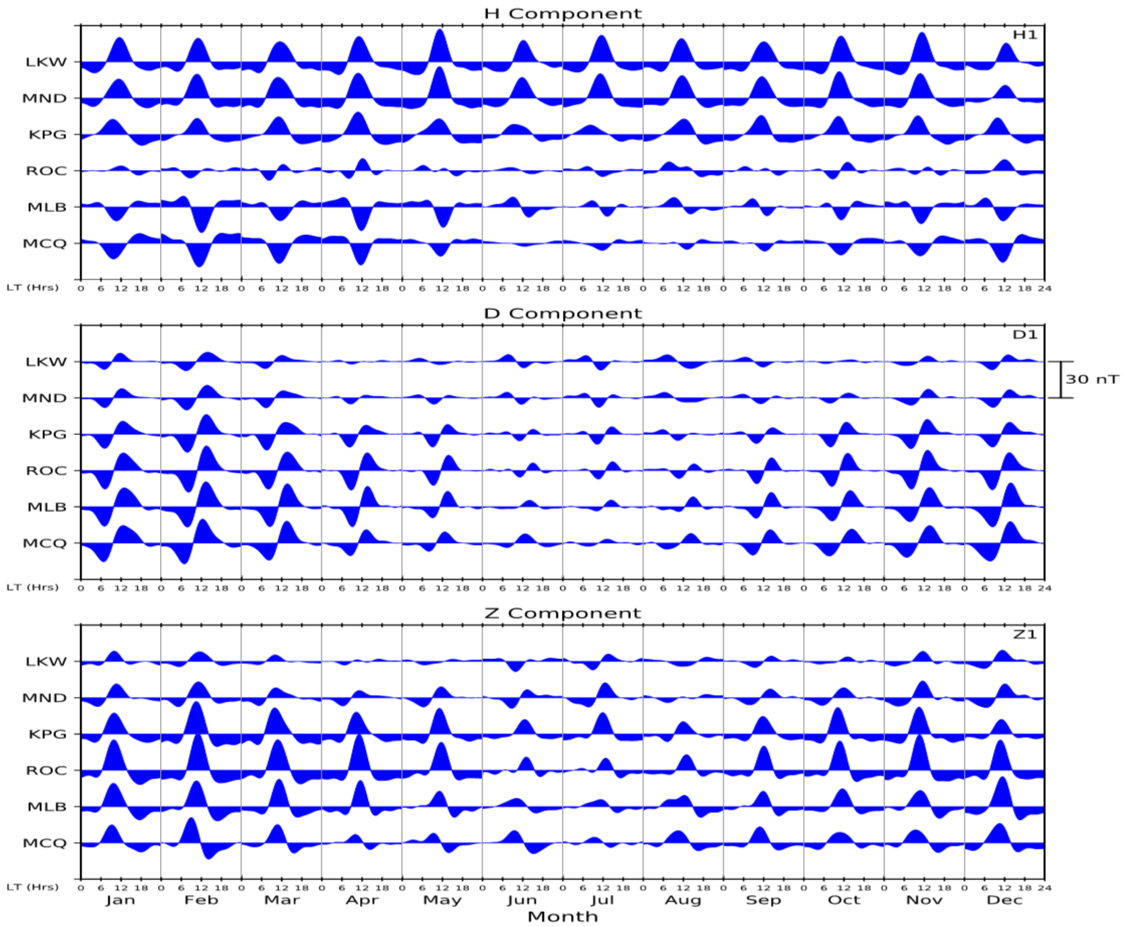

Figure 1: Month-by-month external field variations of the three orthogonal components (H, D, and Z) reconstructed from the spherical harmonic coefficients

Figure 2 shows the internal quiet field variation during dip minimum solar activity year 2008. It is obvious that the internal horizontal quiet field, $MSqH_{int}$ reflect most of the features common to the $MSqH_{ext}$ with similar night-time negative amplitudes that extended to ROC latitude beyond which the amplitudes changed to positive mostly between 16:00 and 06:00 LT hrs as shown in Figure 2 (panel H4). The daytime positive $MSqH_{int}$ amplitudes are apparent at LKW, MND and ROC latitudes thereafter change to negative variations mostly around 06:00 to 16:00 LT hrs at MLB and MCQ latitudes. The daytime maximum positive and negative $MSqH_{int}$ amplitudes $\sim$ 12 nT and $\sim$ -13 nT occurred around 10:00 LT hrs each in February at MND and MCQ latitudes. Generally, the result shows that stations equatorward (poleward) of the ROC are boarded by daytime eastward (westward) current. Also the external $MSqH_{ext}$ magnitudes are about twice greater than their corresponding internal $MSqH_{int}$ magnitudes. The variations of $MSqH_{int}$ change erratically both in phase and magnitudes relative to the $MSqH_{ext}$ magnitudes. The $MSqH_{int}$ erratic behaviour may likely be associated to the electromagnetic induction effect.

Figure 1 (panel D1) illustrate the external eastward quiet field $MSqD_{ext}$ variations. It is apparent in Figure 1 (panel D1) that the $MSqD_{ext}$ is characterized by a pre-noon negative amplitudes between 01:00 and 11:00 LT hrs and afternoon positive magnitudes between 12:00 and 18:00 LT hrs. Similar to what was observed in the Australian region by [18] (see their Figure 2). These features which are mostly seen in (March-September) are expected of stations located in the southern hemisphere. During these periods, the maximum pre-noon (afternoon) $MSqD_{ext}$ amplitudes reached ~ -20 nT (25 nT) around 10:00 (13:00 LT) hrs conspicuously seen each at MLB in December (February). The $MSqD_{ext}$ were generally observed to be stronger (weaker) in summer (winter) month's consistence with earlier observation by [16]. Strangely, the $MSqD_{ext}$ exhibit a form of variation with an "M shape" apparently seen at MND and KPG latitudes in June, July and September. Similar "M Shape" $MSqD_{ext}$ variation has been reported in Australian region by [23]. The salient feature to note in Figure 1 (panel D1) is the conspicuous absence of prominent northward (southward) flow of current during the pre-noon (afternoon) hrs rather a southward (northward) current generating the negative (positive) $MSqD_{ext}$ amplitudes around these periods in May-August at LKW latitudes. These variations are not consistent with the stations located in the southern hemisphere and thus suggest possible intrusion of other mechanisms that distort the $MSqD_{ext}$ variations at LKW latitudes.

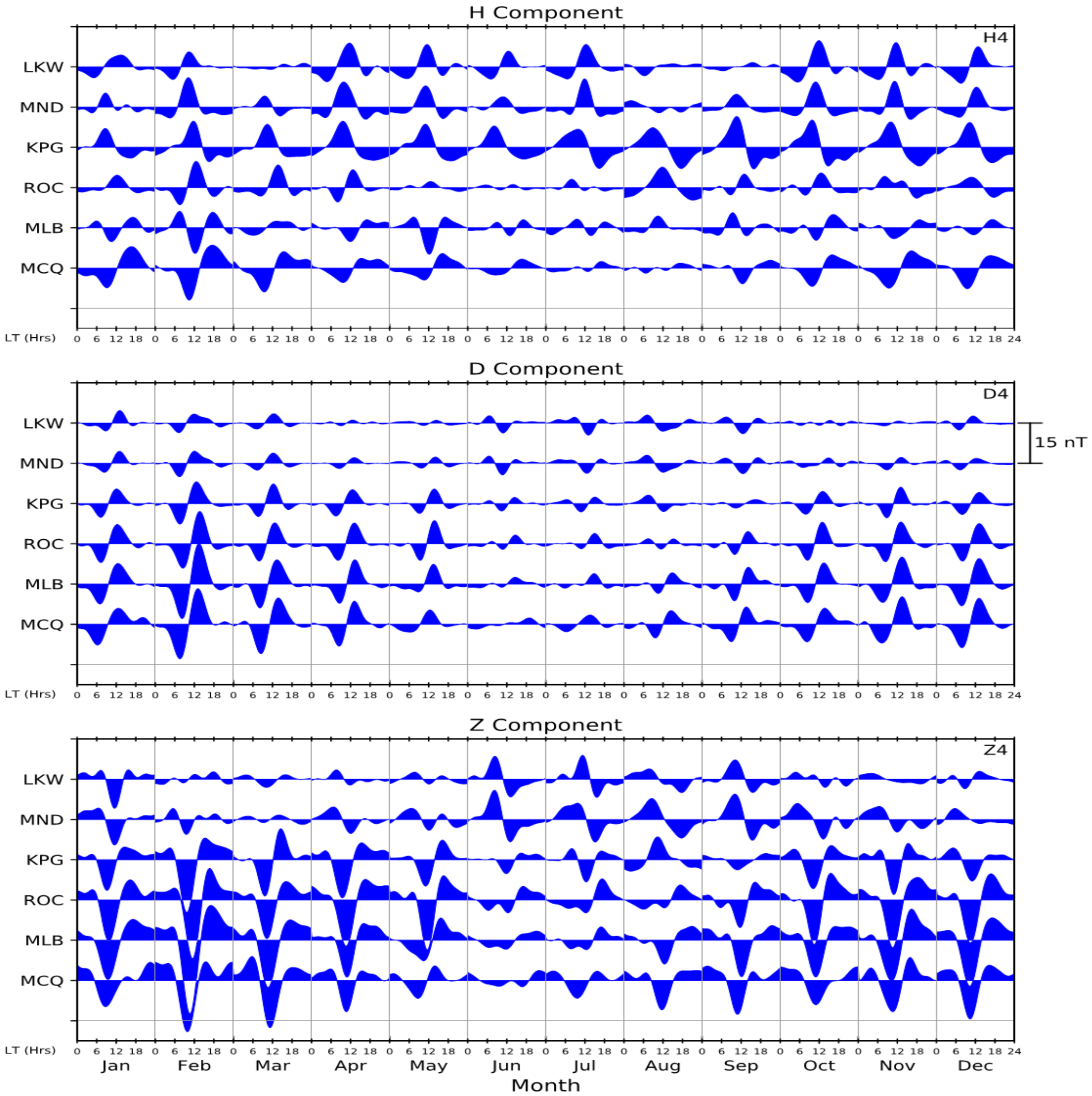

Figure 2 Month-by-month internal field variations of the three orthogonal components (H, D, and Z) reconstructed from the spherical harmonic coefficients

The $MSqD_{int}$ responded well to most of the features common to the $MSqD_{ext}$ amplitudes with similar pre-noon (afternoon) negative (positive) amplitudes in September-April in most latitudes as shown in Figure 2 (panel D4). The pre-noon (afternoon) maximum $MSqD_{int}$ reached ~-14 nT (~ 17 nT) around 08:00 (13:00 LT) hrs each in February at MLB latitude. The variations of $MSqD_{int}$ are not exception to these "M shapes" seen in May-September at LKW and MND with similar appearance in June and July at other latitudes exception of MLB and MCQ (see Figure 2, panel D). Apart of these features, traces of "W shape" are seen in June and July at ROC and MLB latitudes as shown in Figure 2 panel D4. This feature has never been reported (to the best of our knowledge). This effect could possibly arise from the field aligned current. Just like the $MSqD_{ext}$, the $MSqD_{int}$ exhibit higher variations in summer and equinoctial months with much fluctuation in winter months.

Figure 1 (panel Z1) demonstrate the external field variations of the Z-component $MSqZ_{ext}$. The $MSqZ_{ext}$ are characterized by night-time (17:00-06:00 LT) hrs negative variations in most cases and changed to positive amplitudes during the sunlight (07:00-16:00 LT) hrs. These variations are typical of southern hemisphere stations as earlier established by [24]. Exceptions to these variations are LKW and MND with reduced magnitudes that fluctuate particularly in winter months (April-August). The daytime maximum $MSqZ_{ext}$ amplitude ~ 31 nT occurred around 11:00 LT in February at ROC latitude. The $MSqZ_{ext}$ magnitudes generally appeared weaker at LKW located at the magnetic equator and incredibly enhanced at the mid-latitude closer to the Sq focus then deceases afterwards. The daytime positive $MSqZ_{ext}$ amplitudes are stronger during the local summer and equinoctial months (April-September) with exceptional enhancement at KPG and ROC latitudes located closer to the Sq focus.

Figure 2 (panel Z4) illustrate the internal field variations of the Z-component $MSqZ_{int}$ reconstructed from the spherical harmonic coefficients. The $MSqZ_{int}$ exhibit night-time (17:00-05:00 LT) hrs positive amplitudes and daytime (06:00-16:00 LT) hrs negative amplitudes seen across all the latitudes exception of LKW and MND. At these stations (LKW and MND), $MSqZ_{int}$ fluctuate especially in winter months. Apart from these variations, $MSqZ_{int}$ attains its peak ~ -14 nT around 11:00 LT at MLB latitude as depicted in Figure 2 (panel Z4).

Figure 3 illustrate the sum (external plus internal) field variations reconstructed from the spherical harmonic coefficients for each orthogonal component. As shown in Figure 3 (panel J), the sum of the horizontal quiet field $MSqH_{Tot}$ is characterized by a night-time (17:00-05:00 LT) hrs amplitudes and daytime (06:00-16:00 LT) hrs positive amplitudes. These features are particularly seen at LKW, MND and KPG latitudes. The daytime $MSqH_{Tot}$ magnitude significantly reduced with a slight phase variations at ROC latitude thereafter exhibit daytime (night-time) negative (positive) magnitude. During these periods, the daytime maximum $MSqH_{Tot}$ magnitudes for stations equator-ward (pole-ward) of ROC reached ~ 35 nT (~ -30 nT) in May (February) at MND (MCQ) respectively. The daytime positive $MSqH_{Tot}$ amplitudes generally decrease with increasing latitude while the daytime negative amplitude seems to increase with latitudes as demonstrated in Figure 3 (panel J).

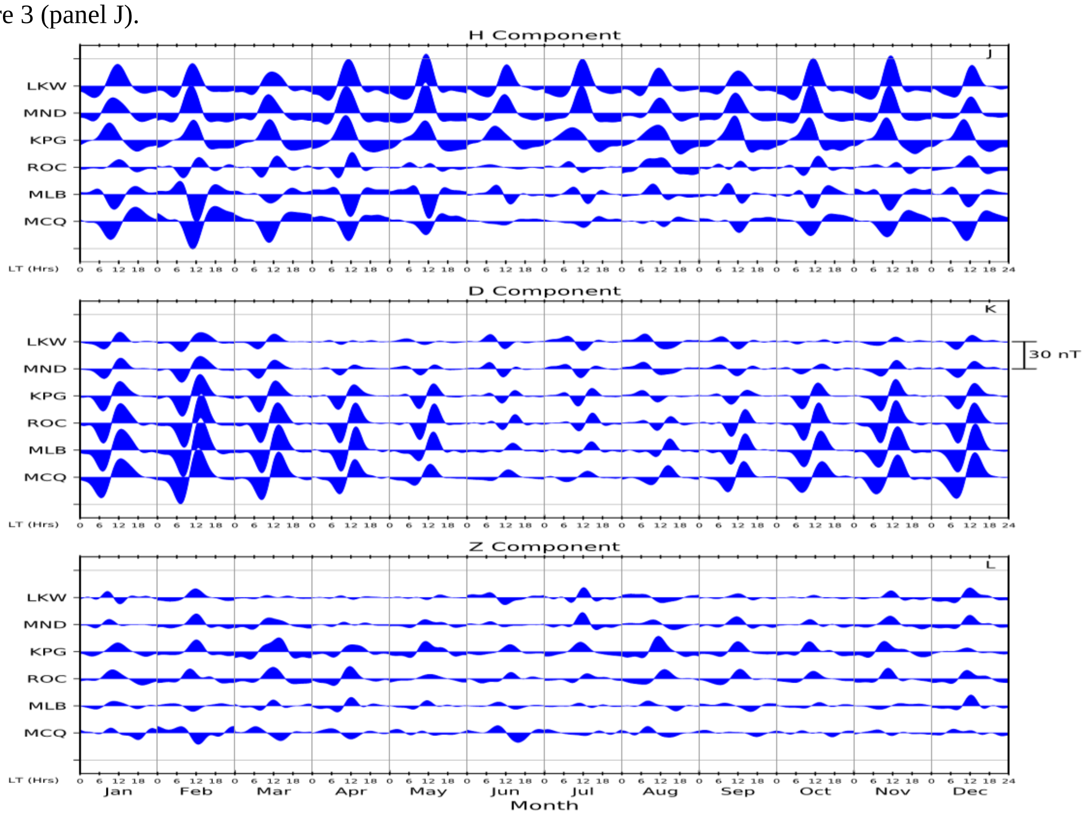

Figure 3 Sum of the quiet monthly field variations reconstructed from the spherical harmonic coefficients

The sum (external plus internal) of the quiet eastward component $MSqD_{Tot}$ shows a northward (southward) current flow producing negative (positive) variations during the pre-noon (afternoon) periods. The maximum pre-noon (afternoon) $MSqD_{Tot}$ reached ~ -30 nT (33 nT) around 07:00 LT (13:00 LT) hrs in February at MCQ (MLB) latitudes. The sum of the field variations of the Z-component reveals the variable pattern of the $MSqZ_{Tot}$ across all the latitudes exception of KPG and ROC. The variable pattern likely indicates the geological effect on the magnetic field record. Despite these variable patterns, the night-time (17:00-05:00 LT) negative $MSqZ_{Tot}$ amplitudes are eminent at KPG and ROC and the positive daytime magnitudes are also seen. The daytime $MSqZ_{Tot}$ peak amplitude ~ 23 nT is seen around 11:00 LT in August at KPG as depicted in Figure 3 (panel L).

Figure 4 illustrate the electrical conductivity-depth profile of the mantle beneath Asia sub-region during the dip minimum solar activity year 2008. The dotted points are estimated conductivity values and the solid line through the conductivity values is the locally regression line fitted to the estimated conductivity-depth values estimated using the Lowess technique [22]. Two conductivity values appeared separately at depth between 370 and 420 km. We are not sure whether they are real values or outliers or perhaps there could be times when the variation of the Sq field is showing some kind of response from small scale high conductivity anomaly at these depth locations.

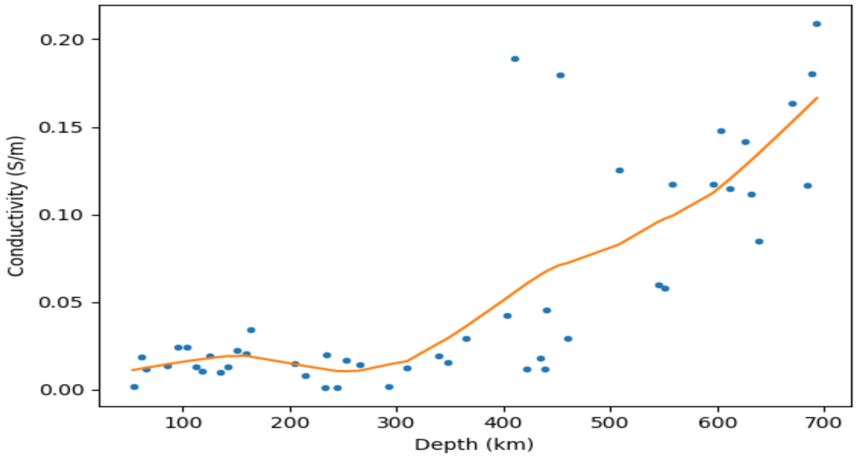

Figure 4: Electrical conductivity profile of the upper mantle beneath Asia sub-region in 2008

Apart from these two conductivity-depth values, generally the conductivity values are much concentrated within the first few kilometers to a depth of about 450 km. Beyond this depth, the density of the conductivity values decreases to a depth of about 680 km. the scattered conductivity values especially at higher depth may result from series of factors that includes: the inherited error from the field measurements, error incurred from spherical harmonic analysis (SHA) fitting, presence of other sources of current such as field-aligned current (FAC). It is imperative to note that even though quietest days are used, the data has some level of noise and the effect of lateral inhomogeneity of which both constitute some level of error that are very difficult to evaluate accurately. As such what we consider as an error is the estimation of the regression fitting for the scattered conductivity values. Despite the scattered conductivity values the lowess fitting mapped out the features of the electrical conductivity from the sub-crustal surface level (~40 km) to a depth of about 680 km in the mantle. The Figure also reveal that the Lowess conductivity profile gradually increases from the sub-crustal surface with an initial magnitude ~0.01 S/m at depth of ~40 km. The conductivity values gradually rose to about 0.02 S/m at ~150 km depth. A substantial decrease in conductivity values to about 0.01 S/m was observed at depth range 240-280 km followed by a sharp increase in conductivity profile to ~0.03 S/m at depth near 320 km (see Figure 4). The conductivity profile steeply rises through the mantle to about 0.07 S/m near 450 km. At depth range between 470 and 520 km there was no evidence of conductivity values to characterize the conductivity of the mantle at this depth range. Similar absence of conductivity values was earlier reported beneath Australia region but at depth between 500 and 750 km, [25]. An evidence of discontinuity was observed at depth of about 380-400 km. generally, the conductivity profile gradually rise through the mantle to a depth of about 680 km without levelling off.

IV. Discussion

The night-time (17:00-05:00 LT) hrs negative $MSqH_{ext}$ at LKW, MND and KPG indicate a well-defined westward current consistent with the dynamo mechanism of the E-region of the ionosphere [6]. The irregular $MSqH_{int}$ variations likely suggest the local electromagnetic induction effect. The reduced daytime positive $MSqH_{ext}$ amplitudes with a slight phase variation at KPG and the subsequent changeover to daytime negative amplitude at ROC suggest the likely position of the external Sq focus nearer to ROC latitude. The salient feature to note is that the daytime positive $MSqH_{ext}$ magnitude at ROC latitude in April, August October and December shows that the external Sq focus in these months are southward (pole-ward) of ROC and remain relatively northward (equator-ward) in other months. This confirmed earlier studies that observed latitudinal movement of the Sq focus e.g., [1, 23, 26]. The significant reduction in $MSqH_{int}$ magnitude at ROC latitude and the daytime reversal of eastward to westward field at MMB as shown in Figure 2 (panel H4) shows the presence of internal Sq focus nearer the MMB latitude. The salient feature to observed is that the internal Sq focus is slightly more pole-ward than the external Sq focus in any of the months through the year. This latitudinal variation between the external and internal Sq focus may likely arise from the electromagnetic induction effect [27].

Generally, the night-time (daytime) $MSqH_{ext}$ and $MSqH_{int}$ variations shows the presence of westward (eastward) currents at low latitudes and changeover to eastward (westward) at mid-latitude region. The magnitudes of the daytime eastward current decreases away from the magnetic equator while its corresponding daytime westward current seems to increase in magnitude from the mid-latitude towards the South Pole. The daytime $MSqH_{ext}$ magnitudes that reached their peak between 10:00 and 13:00 LT hrs are evidence of stronger Sq current caused by intense ionospheric conductivity under the strong influence of solar activity. The variations in local time of their peaks resulted from the prevailing wind system, [28]. The conspicuous variation in $MSqH_{ext}$ amplitudes is an indication of variation in the overhead Sq current system which induces corresponding variations in $MSqH_{int}$ amplitudes. Different mechanisms have been pointed to as the cause of the day-to-day variation of $MSqH_{ext}$ magnitudes. For instance, [2, 6, 28] attributed it to changes in either conductivity or prevailing wind system. As earlier mentioned, $MSqH_{int}$ exhibit features associated with the external field. The magnitude of $MSqH_{int}$ equator-ward of the Sq focus shows slight latitudinal phase variation than those latitudes pole-ward of the Sq focus (see Figure 2 panel H4). These variations may likely be attributed to stronger electromagnetic induction effect.

The observed negative (positive) $MSqD_{ext}$ magnitudes during the pre-noon (afternoon) periods in summer and equatorial months (April-September) depict a well-defined northward (southward) meridional current around these periods [26]. The negative and positive $MSqD_{int}$ amplitude during the pre-noon and afternoon hours in summer and equinoctial month (April-September) is an indication of north-south component of the induced current flow consistent with stations on the southern hemisphere. These variations of $MSqD_{int}$ are no surprised as they are induced by the corresponding $MSqD_{ext}$ variations. Throughout the year, the $MSqD_{ext}$ magnitudes appeared larger than its corresponding $MSqD_{int}$ magnitudes. Their greater magnitudes reflect direct effect of ionospheric conductivity [2] The $MSqD_{ext}$ amplitudes with "W shape" seen particularly in June and July at ROC and MLB latitudes indicate large southward current with smaller northward currents on either side. This produce the relatively large positive $MSqD_{ext}$ amplitudes near noon having smaller pre-noon and afternoon negative amplitude as depicted in Figure 2 (panel D4). The weaker $MSqD_{ext}$ at LKW may be explained as a result of the stations location closer to the magnetic dip equator where the current flow horizontally in the eastward direction during the daytime [29]. The noticeable absence of prominent northward and southward flow of current during the pre-noon and afternoon periods on $MSqD_{ext}$ at LKW latitude in April-September suggest cancellation of the meridional current effect in these months.

The abrupt decrease of $MSqZ_{ext}$ magnitude at LKW latitudes is consistent with the Chapman's theory that the field intensity at the dip equator are flat (zero), since LKW is not exactly at the dip equator it suffered reduced $MSqZ_{ext}$ intensity as shown in Figure 1 (panel Z1). The $MSqZ_{int}$ amplitudes reflect most of the features of the $MSqZ_{ext}$ with higher intensity in summer-equinoctial months. Throughout the year the $MSqZ_{ext}$ are consistently higher than the $MSqZ_{int}$ amplitudes. These greater magnitudes reflect consequences of overhead current and current induce into the conductive solid Earth.

The significant reduction in the intensity and phase shift of $MSqH_{Tot}$ at KPG and the changes in daytime eastward to westward field at ROC suggest likely position of the focal latitudes between KPG and ROC latitudes. The abrupt reduction in $MSqH_{Tot}$ amplitudes at mid-latitude is due to the presence of the Sq focus. Generally, the $MSqD_{Tot}$ exhibit normal variation with a well-defined northward and southward current flow during the pre-noon and afternoon periods. These features which are mostly observed in September-April correspond well with the effect of an ideal Sq current system southerly of the magnetic dip equator. The early occurrence of the pre-noon and afternoon $MSqD_{Tot}$ amplitudes in summer months and later occurrence in winter months reflect the effect of field-aligned currents (FACs). The field-aligned currents (FACs) may likely contribute to the $MSqD_{Tot}$ magnitudes in summer and decrease in winter [30].

The variable pattern of $MSqZ_{ext}$ across all the months in all the stations (exception of KPG and ROC) likely suggest that the magnetic field records may be affected by the geological location of the observations since the vertical component depend on the regional and local anomalies. The phase variations of $MSqZ_{Tot}$ amplitudes from latitude to the other may likely be due to electromagnetic induction effect.

Figure 4 that revealed the conductivity-depth profile of Asia sub-region during the dip minimum solar activity allowed the upper mantle to be viewed as a stack of inhomogeneous spherical layers in variance to the earlier models obtained under the assumption of spherically symmetric Earth [31, 32, 33]. These authors used symmetric distribution model which allows the upper mantle to be viewed as a single homogeneous spherical layer.

It is apparently seen in Figure 4 that the conductivity-depth profile in Asian sub-region is characterized by a downward increase in consistence with earlier findings in Australia, India, Malaysia, Africa and other regions of the world [14, 24, 34, 35, 36[. The downward increase in conductivity is not surprising owing to the fact that the temperature of the Earth's interior increases with depth [37], as such it is expected that the conductivity of the mantle to increase accordingly.

The conductivity values at depth range ~40-100 km showed the existence of weak conductivity zone consistent with findings in the Malaysian region [36]. [38] conducted a laboratory experiment on the conductivity of hydrous olivine to about 0.01 S/m at about 100 km depth similar to what was obtained in the present study. [14] conducted a monumental study on the electrical conductivity of the mantle beneath seven continental region of the world. Their conductivity profile beneath Africa, Central and East Asian sectors is in agreement with the present study at depth range between 50 and 180 km but their result on the Europe, North and South American region are in sharp contrast with the present conductivity profile. They found that beneath Europe and South American region, the conductivity-depth profile increases tremendously. The difference in conductivity of this study with the Europe and South American region may be attributed to lateral inhomogeneity that exists between the continental regions. [36] reported that the conductivity profile within the sub-crustal surface depends on the amount of water content present. Hence, the weak conductivity within the sub-crustal surface may be attributed to the dehydration of the crest through metamorphic processes as earlier pointed out by [39].

The slight enhancement in conductivity profile at depth between 100 and 180 km corresponds to asthenosphere region earlier identified with high conductivity associated with global low seismic velocity, [40]. It is worthy to note that the conductivity of the upper mantle depends on several factors such as the chemical composition, rock type etc. Laboratory experiment earlier conducted showed changes in electrical conductivity of the mantle is associated with changes in the mantle mineral composition [41]. The abrupt increase in conductivity profile at depth near 320 km seems to mark the transition zone and also reflect significant phase changes in the mineral composition of the mantle. Experimental observation by [42] reveals that the most abundant upper mantle rock type is the peridotite. The peridotite is compose of four (4) main minerals; olivine $(M_gFe)_2S_iO_6$ clinopyroxene $Ca(M_gFe)Si_2O_6$ with some aluminous phase (such as plagioclase, spinel or garnet). These authors discussed that phase changes in the upper mantle at a depth range between 300 and 410 km corresponds to a depth at which orthopyrozene transform to clinopyrozene. Hence, we assert that the apparent steep increase in conductivity at 320 km depth in the present study may likely reflect such mantle mineral transformation. The steep rise in conductivity-depth profile between 320 and 500 km of this study corresponds to the mantle transition zone associated with high electrical conductivity, [43].

The evidence of discontinuity at ~380-460 km depth may likely be associated with the transformation of $\alpha -$phase of olivine to β at high temperature and pressure [44]. Generally, the conductivity increase at depth range 350-800 km in the present study is in consonance with the global models that demonstrate increase in conductivity at depth profile 400-800 km and this reflect phase transition of the mantle minerals as identified by previous research workers e.g., [25, 34].

V. Conclusions

Herein we have analysed the magnetic field records during the year of dip minimum solar activity year 2008. The year 2008 still remain the year with the minimal solar activity event for the past 100 years, hence conducive to delineate the features of the external, internal and sum of the Sq fields which are believed to arise from current in the upper atmospheric region and current induced into the conductive Earth structure. The separated Sq fields were further used to estimate the mantle electrical conductivity. The following results were obtained:

1. The $MSqH_{ext}$, $MSqH_{int}$ and $MSqH_{Tot}$ equator-ward of the Sq focus are bounded by daytime (night-time) eastward (westward) currents generating positive (negative) field and opposite variation was observed for stations pole-ward of the Sq focus.

2. A conspicuous absence of prominent northward (southward) current generating negative (positive) $MSqD_{ext}$ amplitudes was observed in May-August at LKW latitude which thus cancellation of meridional effects in these months.
3. The $MSqZ_{ext}$ magnitudes appeared exceptionally large at KNY closer to the Sq focus clearly permitting an inference that the reduction in the source of the $MSqH_{ext}$ amplitudes at PHU closer to the Sq focus cause incredible enhancement on the form of $MSqZ_{ext}$ variation.
4. The noticeable absence of prominent northward and southward current flow at LKW indicates likely intrusion of other current calling the effect of the meridional current at this latitude location.
5. The abrupt reduction of $MSqH_{Tot}$ magnitudes at mid-latitudes is attributed to the presence of the Sq focus and the variable pattern of $MSqZ_{ext}$ suggests influence of geological locations of the study area.
6. The $MSqH_{int}$, $MSqD_{int}$ and $MSqZ_{int}$ magnitudes exhibit slight phase variations that are believed to arise from electromagnetic induction effect.
7. The abrupt increase in conductivity profile at depth near 320 km of this present study mark the transition zone and thus reflect significance phase changes in the mineral composition of the mantle.
8. The conductivity profile reveal various phases of mineral composition and transformation thus summarily indicates lateral inhomogeneous layer bound the Asian sub-region in contrast to the earlier models that reported lateral homogeneous layer.

Author Contributions

The conceptualization of the work was done by Mustapha Abbas and the methodology was designed by Mustapha Abbas and Mukhtar Ibrahim Furfuri. The software application was carried out by Mohammed Bello Kaoje and Mukhrat Mohammed and the validation was done by Aminu Mohammed and Aminu Yusuf Koko. The First draft copy of the manuscript was prepared by Mustapha Abbas, reviewed by Yoshikawa Akimoto.
All authors have read and agreed to the published version of the manuscript.

Funding

This work received no external funding.

Acknowledgments

The authors acknowledge all of MAGDAS hosts for maintaining our instrument whose magnetic field records are used in this study.

Conflicts of Interest

The authors declare no conflict of interest.

References

[1] Vichare, G., Rawat, R., Jadhav, M. and Sinha, A.K., 2017. Seasonal variation of the Sq focus position during 2006–2010. *Advances in Space Research*, *59*(2), pp.542-556. https://doi.org/10.1016/j.asr.2016.10.009

[2] Abbas, M., Abidin, Z.Z., Jusoh, M.H., Bolaji, O.S. and Yoshikawa, A., 2019. Features of horizontal magnetic field intensity over northern island of Malaysia. *Indian Journal of Physics*, *93*(10), pp.1247-1257. https://doi.org/10.1007/s12648-019-01388-9

[3] Chapman, S., & Bartels, J. (1940). Geomagnetism, 1049 pp: Oxford Univ. Press, New York.

[4] Gauss, C. (1841). General theory of terrestrial magnetism, English translation in Scientific Memoirs, edited by R: Taylor

[5] Winch, D. E. (1981), Spherical harmonic analysis of geomagnetic tides, 1964–1965, Philos. Trans. R. Soc. A, 303, 1–104. https://doi.org/10.1098/rsta.1981.0193

[6] Yamazaki, Y. and Maute, A., 2017. Sq and EEJ—a review on the daily variation of the geomagnetic field caused by ionospheric dynamo currents. *Space Science Reviews*, *206*(1), pp.299-405. https://doi.org/10.1007/s11214-016-0282-z

[7] Liu, X., Han, P., Hattori, K., Chen, H., Yoshino, C., Zhao, X., et al. (2021). Seasonal variation characteristics of geomagnetic *S*q external and internal equivalent current systems in East- Asia and Oceania regions. *Journal of Geophysical Research: Space Physics*, *126*, e2021JA029113. https://doi.org/10.1029/2021JA029113

[8] Campbell, W. H., Arora, B. R., & Schiffmacher, E. R. (1993). External Sqcurrents in the India-Siberia region. *Journal of Geophysical Research: Space Physics*, *98*(A3), 3741-3752. https://doi.org/10.1029/92JA02552

[9] Liu, X., Hattori, K., Han, P., Chen, H., Chie, Y., & Zhao, X. (2019). Possible anomalous changes in solar quiet daily geomagnetic variation (Sq) Related to the 2011 off the Pacific coast of Tohoku Earthquake (Mw 9.0). Pure and Applied Geophysics, 176, 1–14. https://doi.org/10.1007/s00024-018-02086-z

10] Fukushima, N. (1979). Electric potential difference between conjugate points in middle latitudes caused by asymmetric dynamo in the ionosphere. *Journal of geomagnetism and geoelectricity*, *31*(3), 401-409. https://doi.org/10.5636/jgg.31.401

[11] Takeda, M. (2002a). The correlation between the variation in ionospheric conductivity and that of the geomagnetic Sq field. *Journal of Atmospheric and Solar-Terrestrial Physics*, *64*(15), 1617-1621. https://doi.org/10.1016/S1364-6826(02)00140-2

[12] Park, J., Yamazaki, Y., & Lühr, H. (2020). Latitude dependence of inter-hemispheric field aligned currents (IHFACs) as observed by the Swarm constellation. *Journal of Geophysical Research: Space Physics*, *125*, e2019JA027694. https://doi.org/10.1029/2019JA027694

[13] Yamashita, S., & Iyemori, T. (2002). Seasonal and local time dependences of the interhemispheric field-aligned currents deduced from the Ørsted satellite and the ground geomagnetic observations. *Journal of Geophysical Research: Space Physics, 107*(A11). https://doi.org/10.1029/2002JA009414

[14] Cambell, W. H., & Schiffmacher, E. R. (1988). Quiet ionospheric currents of the southern hemisphere derived from geomagnetic records. *Journal of Geophysical Research: Space Physics, 93*(A2), 933-944. https://doi.org/10.1029/JA093iA02p00933

[15] Pedatella, N. M., Forbes, J. M., & Richmond, A. D. (2011). Seasonal and longitudinal variations of the solar quiet (Sq) current system during solar minimum determined by CHAMP satellite magnetic field observations. *Journal of Geophysical Research: Space Physics, 116*(A4), n/a-n/a. https://doi:10.1029/2010ja016289

[16] Stening, R. J., & Winch, D. E. (2013). The ionospheric Sq current system obtained by spherical harmonic analysis. *Journal of Geophysical Research: Space Physics, 118*(3), 1288-1297. https://doi.org/10.1002/jgra.50194

[17] Campbell, W. H., & Schiffmacher, E. R. (1986). A comparison of upper mantle subcontinental electrical conductivity for North America, Europe, and Asia. *Journal of Geophysics - Zeitschrift fur Geophysik, 59*(1), 56-61.

[18] Campbell, W. H., & Schiffmacher, E. R. (1987). Quiet ionospheric currents and earth conductivity profile computed from quiet-time geomagnetic field changes in the region of Australia. *Australian journal of physics, 40*(1), 73-88. https://doi.org/10.1071/PH870073

[19] Schmucker, U. (1970). Anomalies of geomagnetic variations in the southwestern United States. *Bull. Scripps. Inst. Oceanogr., 13*, 1-165.

[20] Campbell, W. H., & Anderssen, R. S. (1983). Conductivity of the subcontinental upper mantle: an analysis using quiet-day geomagnetic records of North America. *Journal of geomagnetism and geoelectricity, 35*(10), 367-382. https://doi.org/10.5636/jgg.35.367

[21] Campbell, W. H. (2003). *Introduction to geomagnetic fields*: Cambridge University Press.

[22] Cleveland, W. S. (1979). Robust Locally Weighted Regression and Smoothing Scatterplots. *Journal of the American Statistical Association, 74*(368), 829–836. https://doi.org/10.1080/01621459.1979.10481038

[23] Stening, R., Reztsova, T., & Minh, L. H. (2005). Day-to-day changes in the latitudes of the foci of the Sq current system and their relation to equatorial electrojet strength. *Journal of Geophysical Research: Space Physics, 110*(A10). https://doi.org/10.1029/2005JA011219

[24] Chapman, S. (1919). I. The solar and lunar diurnal variations of terrestrial magnetism. *Phil. Trans. R. Soc. Lond. A, 218*(561-569), 1-118. https://doi.org/10.1098/rsta.1919.0001

[25] Campbell, W. H., Barton, C. E., & Welsh, W. (1998). Quiet-day ionospheric currents and their application to upper mantle conductivity in Australia. *Earth, Planets and Space, 50*(4), 347-360. https://doi.org/10.1186/BF03352121

[26] Stening, R., & Reztsova, T. (2007). Variation of Sq focus latitudes in the Australian/Pacific region during a quiet sun year. *Journal of Atmospheric and Solar-Terrestrial Physics, 69*(6), 734-740. https://doi.org/10.1016/j.jastp.2006.12.002

[27] Campbell, W. H., & Schiffmacher, E. R. (1985). Quiet ionospheric currents of the northern hemisphere derived from geomagnetic field records. *Journal of Geophysical Research: Space Physics, 90*(A7), 6475-6486. https://doi.org/10.1029/JA090iA07p06475

[28] Okeke, F., & Hamano, Y. (2000). Daily variations of geomagnetic HD and Z-field at equatorial latitudes. *Earth, Planets and Space, 52*(4), 237-243. https://doi.org/10.1186/BF03351632

[29] Chapman, S. (1951). The equatorial electrojet as detected from the abnormal electric current distribution above Huancayo, Peru, and elsewhere. *Archiv Fuer Meteorologie, Geophysik und Bioklimatologie, Serie A, 4*(1), 368-390. https://doi.org/10.1007/BF02246814

[30] Thu, H. P. T., Amory-Mazaudier, C., & Le Huy, M. (2011). *Sq field characteristics at Phu Thuy, Vietnam, during solar cycle 23: comparisons with Sq field in other longitude sectors.* Paper presented at the Annales Geophysicae.

[31] Banks, R. (1972). The overall conductivity distribution of the Earth. *Journal of geomagnetism and geoelectricity, 24*(3), 337-351. https://doi.org/10.5636/jgg.24.337

[32] Faynberg, E., & Rotanova, N. (1975). Distribution of electrical conductivity and temperature in the interior of the Earth according to deep electromagnetic sounding. *Geomagnetism and Aeronomy, 14*, 603.

[33] Hobbs, B. (1987). Conductivity profiles from global data *Electrical Properties of the Earth's Mantle* (pp. 393-407): Springer.

[34] Arora, B. R., Campbell, W. H., & Schiffmacher, E. R. (1995). Upper mantle electrical conductivity in the Himalayan region. *Journal of geomagnetism and geoelectricity, 47*(7), 653-665. https://doi.org/10.5636/jgg.47.653

[35] Obiora, D. N., Okeke, F. N., & Yumoto, K. (2015). Electrical conductivity of mantle in the North Central region of Nigeria. *Journal of African Earth Sciences, 101*, 274-281. https://doi.org/10.1016/j.jafrearsci.2014.10.002

[36] Abidin, Z. Z., Jusoh, M. H., Abbas, M., & Yoshikawa, A. (2018). Application of solar quiet (Sq) current in determining mantle conductivity-depth structure in Malaysia. *Journal of Atmospheric and Solar-Terrestrial Physics*. https://doi.org/10.1016/j.jastp.2018.01.019

[37] Tozer, D. (1970). Temperature, Conductivity, Composition and Feat Flow. *Journal of geomagnetism and geoelectricity, 22*(1-2), 35-51. https://doi.org/10.5636/jgg.22.35

[38] Yoshino, T., & Katsura, T. (2013). Electrical conductivity of mantle minerals: role of water in conductivity anomalies. *Annual Review of Earth and Planetary Sciences, 41*, 605-628. https://doi.org/10.1146/annurev-earth-050212-124022

[39] Hyndman, R., & Hyndman, D. (1968). Water saturation and high electrical conductivity in the lower continental crust. *Earth and Planetary Science Letters, 4*(6), 427-432. https://doi.org/10.1016/0012-821X(68)90017-4

[40] Dziewonski, A. M., & Anderson, D. L. (1981). Preliminary reference Earth model. *Physics of the Earth and Planetary Interiors, 25*(4), 297-356. https://doi.org/10.1016/0031-9201(81)90046-7

[42] Xu, Y., Shankland, T. J., & Poe, B. T. (2000). Laboratory-based electrical conductivity in the Earth's mantle. *Journal of Geophysical Research: Solid Earth, 105*(B12), 27865-27875. https://doi.org/10.1029/2000JB900299

[43] Utada, H., Koyama, T., Shimizu, H., & Chave, A. (2003). A semi-global reference model for electrical conductivity in the mid-mantle beneath the north Pacific region. *Geophysical Research Letters, 30*(4). https://doi.org/10.1029/2002GL016092

[44] Katsura, T., & Ito, E. (1989). The system Mg2SiO4-Fe2SiO4 at high pressures and temperatures: Precise determination of stabilities of olivine, modified spinel, and spinel. *Journal of Geophysical Research: Solid Earth, 94*(B11), 15663-15670. https://doi.org/10.1029/JB094iB11p15663